Quantitative analysis of the perfusion in the kidneys, liver, pancreas, small intestine and mesenteric lymph nodes in healthy cats using contrast enhanced ultrasound

Leinonen, Merja Riitta

2010

þÿ L e i n o n e n , M R , R a e k a l l i o , M , V a i n i o , O , R u o h o n i e m i , M , B i l l e r ,
2010 , ' Quantitative analysis of the perfusion in the kidneys, liver, pancreas, small intestine
and mesenteric lymph nodes in healthy cats using contrast enhanced ultrasound ' ,
þÿ A m e r i c a n J o u r n a l o f V e t e r i n a r y R e s e a r c h , v o l 7 1 , n o . 1 1 , p p . 1 3 0 5 1

http://hdl.handle.net/10138/18548

Quantitative contrast-enhanced ultrasonographic analysis of perfusion in the kidneys, liver, pancreas, small intestine, and mesenteric lymph nodes in healthy cats

Merja R. Leinonen, DVM; Marja R. Raekallio, DVM, PhD; Outi M. Vainio, DVM, PhD; Mirja O. Ruohoniemi, DVM, PhD; David S. Biller, DVM; Robert T. O'Brien, DVM, MS

Objective—To evaluate perfusion of abdominal organs in healthy cats by use of contrast-enhanced ultrasonography.

Animals—10 young healthy anesthetized cats.

Procedures—Contrast-enhanced ultrasonography of the liver, left kidney, pancreas, small intestine, and mesenteric lymph nodes was performed on anesthetized cats.

Results—Typical perfusion patterns were found for each of the studied organs. Differences in perfusion among organs were associated with specific physiologic features. The liver was enhanced gradually and had a more heterogeneous perfusion pattern because of its dual blood supply and close proximity to the diaphragm, compared with other organs. An obvious and significant difference in perfusion was detected between the renal cortex and medulla. No significant differences in perfusion were detected among the pancreas, small intestine, and mesenteric lymph nodes.

Conclusions and Clinical Relevance—Results indicated that contrast-enhanced ultrasonography can be used in cats to estimate organ perfusion as in other species. Observed differences in perfusion variables can be mostly explained by physiologic differences in vascularity. (*Am J Vet Res* 2010;71:1305–1311)

In CEUS, the contrast agent is given IV and is purely intravascular. The contrast agent consists of gas-filled microbubbles encapsulated by a shell of various compositions and is detectable in circulation for several minutes. The microbubbles resonate when insonated via ultrasonography, generating echoes at twice the frequency (second harmonics) of the transmitted ultrasonographic impulse. For the detection of real-time perfusion in tissues, a specialized contrast-specific ultrasonography technique (eg, harmonic and coded imaging or phase amplitude modulation) is needed to visualize these returning echoes, allowing detection of tissue microcirculation.

Compared with older Doppler techniques, detection of lesion perfusion is better with CEUS because Doppler techniques are prone to several artifacts and cannot detect small vessels, slow, low-volume blood flow, or flow from unfavorable angles.[1]

Contrast-enhanced ultrasonography can be used to evaluate tissue microcirculation qualitatively or quantitatively. In qualitative analysis, the tissues' macro- and microvascular structure can be visualized in real time. In quantitative analyses, detailed information of signal intensity versus time can be obtained from a selected ROI, resulting in several perfusion variables acquired from the generated time-intensity curve.[2] Therefore, by

Abbreviations

AT	Arrival time
BI	Baseline intensity
CEUS	Contrast-enhanced ultrasonography
CT	Computed tomography
MRI	Magnetic resonance imaging
PI	Peak intensity
ROI	Region of interest
TTPinj	Time to peak from injection
TTPinr	Time to peak from initial rise
Wi	Wash-in rate
Wo	Wash-out rate

Received June 23, 2009.
Accepted October 8, 2009.
From the Department of Equine and Small Animal Medicine, Faculty of Veterinary Medicine, University of Helsinki, FIN-00014 Helsinki, Finland (Leinonen, Raekallio, Vainio, Ruohoniemi); the Department of Clinical Sciences, College of Veterinary Medicine, Kansas State University, Manhattan, KS 66506 (Biller); and the Department of Veterinary Clinical Medicine, College of Veterinary Medicine, University of Illinois, Champaign-Urbana, IL 61802 (O'Brien).
Supported by the Orion-Farmos Research Foundation, Helvi-Knuuttila Trust, and Finnish Veterinary Foundation.
Presented in part as a poster at the Annual Meeting of the European Association of Diagnostic Imaging, Svolvaer, Norway, August 2008, and in part as an abstract at the Annual Meeting of the International Veterinary Radiology Association, Búzios, Brazil, July 2009.
The authors thank Hannu Rita for statistical assistance.
Address correspondence to Dr. Leinonen (merja.leinonen@helsinki.fi).

use of CEUS, tissue perfusion can be estimated as the concentration of microbubbles in the blood flow (signal intensity), indicating quantity of blood flow.[3,4]

Perfusion of a tissue may vary with diseases, such as neoplasia, trauma, and infarction. These perfusional changes in organ parenchyma can be detected with CEUS, which can improve disease characterization. Contrast-enhanced ultrasonography was introduced to human medicine as a new method for detecting focal changes in perfusion of several abdominal organs, including liver, spleen, kidneys, and pancreas.[5,6] It is also used in detecting pathological changes affecting large vessels[7] and in diagnosing abdominal trauma.[8] Contrast-enhanced ultrasonography is important not only in detecting perfusional changes and aiding diagnosis of neoplastic, traumatic, and necrotic lesions, but also in the treatment and monitoring of cancer.[9] Most studies have focused on the liver. Liver lesions can be diagnosed with high accuracy as benign or malignant by use of CEUS, even up to the histologic level.[7,10]

Contrast-enhanced ultrasonography is considered to be nearly as reliable a diagnostic tool as CT and MRI in medicine.[11,12] Computed tomography and MRI are presently the gold standard for imaging malignancies in human medicine. The possible adverse effects, including adverse or allergic reactions and potential nephrotoxicity of the iodine- and gadolinium-containing contrast agents used in those techniques, limit their use, particularly in patients with kidney disease.[13,14] The use of CT and MRI for evaluation of masses and tumors has been studied to a certain extent in veterinary medicine.[15,16] In addition to the posibility of contrast-induced toxicoses, the requirement for anesthesia limits the use of CT and MRI in veterinary medicine, which makes CEUS a valuable alternative.

Contrast-enhanced ultrasonography has been proven to be a safe and minimally invasive diagnostic tool for dogs,[17–21] cats,[22] and humans.[23,24] In dogs, reports exist about quantitative[17–21] and qualitative[25–29] studies that used contrast-enhanced harmonic imaging techniques. One quantitative study[22] was performed on cats and used contrast-enhanced power and color Doppler techniques to assess vascularity and blood flow in the pancreas. The only current clinical indication for use of CEUS in veterinary medicine is detection and characterization of focal lesions in the liver and spleen in dogs.[25–29] The purpose of the study reported here was to evaluate the perfusion of normal organs in healthy anesthetized cats by use of CEUS, to serve as a reference for later clinical studies.

Materials and Methods

Study population—The study was performed at the College of Veterinary Medicine, Kansas State University. Ten healthy young (5 to 6 months of age) sexually intact male domestic shorthair cats weighing 3.58 to 4.26 kg were included in the study. Clinical examinations were performed on each cat along with CBCs and a serum biochemical panel to exclude metabolic disease. Urinalysis and bacteriologic culture of urine were performed to exclude cats with infections or hematuria. The cats were premedicated with atropine (0.02 mg/kg, SC) and sedated with acepromazine (0.06 to 0.1 mg/kg, SC) and morphine (0.25 to 0.5 mg/kg, SC), and general anesthesia was induced with diazepam (0.3 mg/kg, IV) and ketamine (6 mg/kg, IV). While each cat was anesthetized, a 25-gauge IV catheter was placed in a cephalic vein. The indication for anesthesia was concurrent neutering.

The cats used in this study were purpose-bred laboratory cats used earlier in another research project at the College of Veterinary Medicine, Kansas State University. The protocol was planned so that the study could be conducted simultaneously with the neutering procedure done for the cats in the other research study. The protocol was approved by the Institutional Animal Care and Use Committee.

Ultrasonography—Ultrasonography was performed by use of an 8- to 15-MHz linear transducer, with a transmit frequency of approximately 7 MHz, on an ultrasonography machine[a] with contrast-specific software.[b] The hair was clipped over the ventrolateral portion of the abdomen. Alcohol and gel were applied to the skin, and the transducer was manually positioned by the same person during each imaging procedure. Care was taken to keep the transducer in the corresponding location and depth for each organ group. A mechanical index was maintained at 0.31 to 0.33 depending on depth of view, which is an intermediate mechanical index that results in image optimization for the selected transmit frequency, machine system, and contrast medium. Standardized parameters included depth (3 cm for the pancreas, small intestine, and lymph node; 4.5 cm for the liver, renal cortex, and medulla), time gain compensation, overall gain, and focal zones. Two focal zones were placed at the level of or just below the organ imaged for each organ group. The number and placement of focal zones were optimized for better image quality with the selected transducer frequency and imaging depth. Organs were imaged in the following order: liver, left kidney, pancreas, small intestine, and mesenteric lymph nodes. The left kidney, left lobe of the liver, and pancreas were imaged separately in the sagittal plane of the cat. The small intestine and mesenteric lymph nodes were imaged simultaneously in the transverse plane. All cats received 1 to 2 bolus injections (0.1 mL for each injection) of contrast medium,[c] followed by a bolus of 0.5 mL of heparinized saline (0.9% NaCl) solution for each imaged organ. The injections were given in a standardized manner by the same person throughout the study. A digital imaging series of 30 seconds with a frame rate of 16 to 22 Hz, depending on the depth of the organ imaged, was recorded after each contrast injection. The time between the injections was approximately 2 minutes or until no contrast medium was visible. Between each injection, residual bubbles were destroyed by continuous scanning of the imaged organ, cranial portion of the abdomen, and aorta with fundamental ultrasonography and output power adjusted to 100%, until background echogenicity was similar to that seen before injection. Time-intensity curves were created online from the raw imaging data[d] and exported and evaluated with an external computer by use of commercial software.[e,f]

Image analysis and descriptive statistics—Standardized time-intensity curves were created from se-

lected ROIs in each organ (**Figure 1**), representing the signal intensity (decibels) in relation to time (seconds). Care was taken not to include any adjacent tissues (eg, mesentery or falciform ligament fat) or larger vessels inside the ROI. In the pancreas, small intestine, and mesenteric lymph nodes, the size of the ROI was chosen so that it covered the organ parenchyma as well as possible. However, it was limited in size when avoiding large vessels near the organ of interest. Artifactual data, such as data from adjacent tissues that moved into the ROI during respiratory motion, were removed. In the liver, placement of the ROI was left from midline, but the placement varied slightly among individuals because of respiratory motion and image quality.

The functional perfusion variables[2,20] (**Figure 2**) chosen for analysis were AT, defined as the time point when contrast level is increasing to greater than baseline in the time-intensity curve, followed by a further rise; TTPinj; BI, defined as the signal intensity during AT; PI, during TTPinj; TTPinr (TTPinj-AT); Wi; and Wo. Wash-in rate and Wo were calculated as the maximal change rate, measured approximately at 10% greater than baseline and 90% from the peak, respectively, according to the following guidelines: Wi was 10% greater than the highest point of the baseline noise (10% greater than baseline), where all subsequent points continued to increase to a point along the same contiguous line that reached 90% of the maximum value (90% of the peak). The data were then regressed for that data set for significance of linearity. The slope of the line of the regressed data set was used for the Wi. Wash-out rate was determined from a point 90% of the maximum point, where all subsequent points continued to decrease, to the final point measured (for liver and renal medulla) or until the points reached 20% of the previous baseline value. The data were then regressed for significance of linearity. The slope of the line of the regressed data set was used for the Wo. For both Wi and Wo, noise was defined as points or sets of points not within the regressed line that were removed from the final data set. The liver, renal cortex, and renal medulla were imaged in all 10 cats. The pancreas, small intestine, and mesenteric lymph nodes were imaged in only 8 cats. Wash-out rate could be calculated in only 9 cats in the renal medulla because of a gradual sloping during the 30-second time interval. In 1 cat, washing out of renal medulla was gradual and could not be measured within the first 30 seconds. Wash-out rate in the

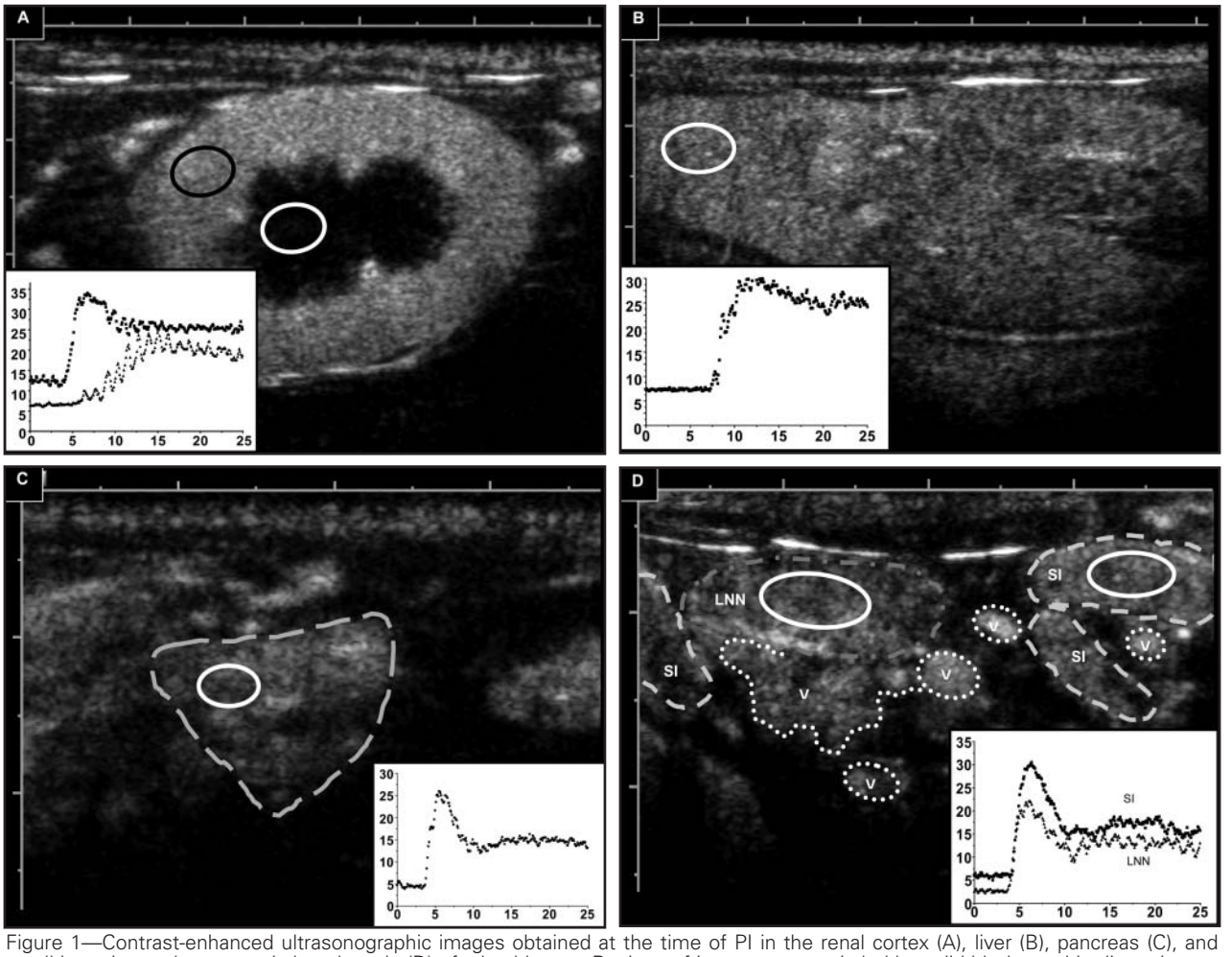

Figure 1—Contrast-enhanced ultrasonographic images obtained at the time of PI in the renal cortex (A), liver (B), pancreas (C), and small intestine and mesenteric lymph node (D) of a healthy cat. Regions of interest are encircled by solid black or white lines. In part C, the outline of the pancreas is indicated by a dashed line. In part D, the small intestine (SI), lymph node (LNN), and vessels (V) are encircled by dashed or dotted lines. Inset graphs provide corresponding time intensity curves (x-axis = time [seconds]; y-axis = intensity [decibels]) from the ROIs.

pancreas was calculated in 7 cats because of bad image quality in 1 cat.

In 8 cats, the data of the liver and renal cortex were obtained by determining the mean of 2 injections. In the other 2 cats, the second recording and corresponding time-intensity curve were rejected because of poor image quality. In the data of the renal medulla (n = 10 cats), pancreas (8), small intestine (8), and mesenteric lymph nodes (8), only 1 recording with corresponding time-intensity curve was available; therefore, direct measurements were used instead of means.

Statistical analysis—Data calculated for each variable included means and SDs. Statistical analysis was made with statistical software[g,h]; ANOVA with repeated measurements was used to compare variables among cats within each organ. The variances within and among cats in the liver and renal cortex were analyzed with the Student *t* test with 2-tailed *P* values and 1-sample *t* test of the difference between 2 injections. Analysis of variance with repeated measurements and Student *t* test were used to compare variables among organs or organ groups within cats. Subgroups of small intestine, mesenteric lymph nodes, and pancreas were compared because these organs have the most similarities in circulation. For this purpose, ANOVA and post hoc Student *t* tests with Bonferroni correction were performed. The remaining organs were compared by use of the Student *t* test, as follows: the liver was compared with renal cortex, pancreas, and small intestine, and the renal cortex was compared with the liver, pancreas, and small intestine. The same organs or organ subgroups were also tested by use of the Pearson correlation test to determine whether similar correlations existed in the variables among the organs within the same cat. Coefficient variation was used to estimate the amount of internal variation in the perfusion variables analyzed. Significance for analysis was set at $P < 0.05$.

Results

Subjective results—Enhancement of the different organs varied in time and pattern (Figure 1). Applying contact between the linear transducer and the cat was somewhat difficult and required a moderate amount of pressure, especially when the liver was being imaged. The image quality was therefore not always optimal for imaging the entire liver. After injection of the contrast agent, there was an immediate subsequent enhancement of hepatic arteries and portal veins to a great extent. This was followed by more gradual enhancement of the liver parenchyma. In general, the image was considered more heterogeneous in the liver than in the other organs.

The renal parenchyma was enhanced in 2 phases: the contrast agent arrived first in the cortex, followed by a more gradual and sparsely spotted enhancement of the medulla (Figure 1). The enhancement of cortex and medulla reached almost equal intensity at 30 seconds; by this time, the cortex was already in wash-out phase.

The pancreas, small intestine, and mesenteric lymph nodes all were enhanced early and intensely immediately after the large supplying vessels were enhanced (Figure 1). Keeping the ROI in the middle of the scanned area, thereby avoiding larger vessels and adjacent tissues, was more difficult in the liver and pancreas, the organs most affected by respiratory motion.

Descriptive results—The numeric results describing the perfusion of all the organs were analyzed (**Table 1**). All data included in the study were significantly correlated in a linear regression.

Repeatability—Variation tested within cats between the 2 injections was not larger than the variation among cats. In the liver data, however, a significant ($P = 0.014$) difference was detected in the BI between the injections.

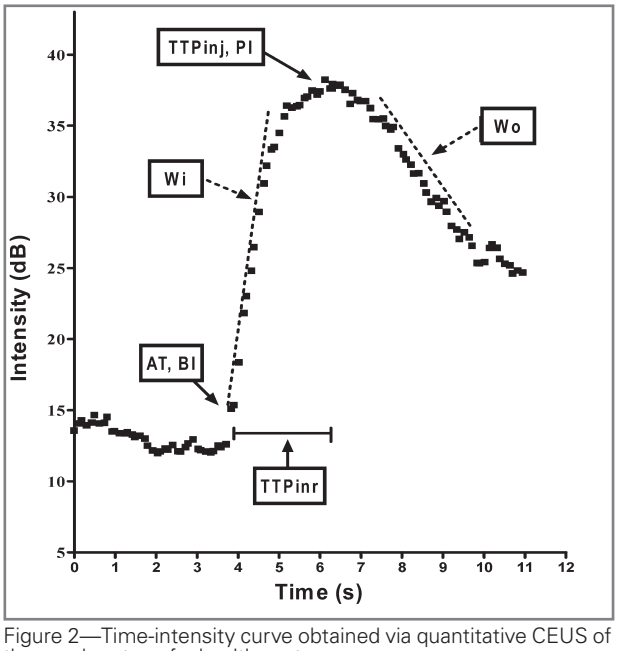

Figure 2—Time-intensity curve obtained via quantitative CEUS of the renal cortex of a healthy cat.

Table 1—Results (mean ± SD) of quantitative CEUS of various organs in healthy cats.

Organ	AT (s)	BI (dB)	TTPinj (s)	PI (dB)	TTPinr (s)	Wi (dB/s)	Wo (dB/s)
Renal cortex	3.96 ± 0.52*†‡	10.10 ± 3.52†	5.99 ± 0.61*†‡	32.40 ± 4.96†	2.03 ± 0.45*†‡	12.20 ± 2.38*†	–3.12 ± 0.76*†‡
Renal medulla	8.08 ± 2.76§	7.46 ± 1.40§	21.80 ± 11.10§	16.00 ± 5.75§	13.7 ± 9.79§	1.48 ± 2.04§	–0.13 ± 0.06§
Liver	5.81 ± 1.96‡§‖	10.40 ± 3.62§‖	9.66 ± 2.90‡§‖	29.70 ± 3.15§‖	3.86 ± 1.32‡§‖	5.89 ± 3.38‡§‖	–0.23 ± 0.08‡§‖
Pancreas	4.10 ± 0.47*	6.19 ± 1.97*	5.96 ± 0.85*	23.80 ± 4.96*	1.86 ± 0.86*	11.43 ± 4.92*	–4.03 ± 2.10*
Small intestine	4.38 ± 0.46*†	7.79 ± 2.44	6.47 ± 2.44*§	27.60 ± 5.02	2.1 ± 0.31*§	10.83 ± 2.96*	–3.08 ± 1.21*
Lymph node	4.20 ± 0.61*	5.85 ± 2.89	6.37 ± 0.74*	23.60 ± 4.37	2.17 ± 0.45*	9.30 ± 2.45*	–2.79 ± 0.86*

Significant ($P < 0.05$) differences in perfusion variables among organs (*Liver; †Renal medulla; ‡Small intestine; §Renal cortex; ‖Pancreas) are indicated by superscript symbols.

Comparison of perfusional variables among organs—Differences between the renal cortex and medulla were significant for all perfusion variables (Table 1). In the subgroup of small intestine, lymph nodes, and pancreas, no significant differences were observed after post hoc testing and the Bonferroni correction. The liver differed from the renal cortex and pancreas in all perfusion variables. Between the liver and small intestine, a significant difference was detected in all variables except BI and PI. Moreover, a significant correlation was detected between the small intestine and lymph nodes in AT ($r = 0.943$), BI ($r = 0.734$), and TTPinj ($r = 0.856$) and between the renal cortex and small intestine in AT ($r = 0.822$) and TTPinj ($r = 0.938$).

Coefficient of variation—The variation measured as the coefficient of variation was not large (< 25%) in any of the studied organs in the PI, with the exception of the renal medulla. Much variation (> 30%) occurred in BI in all studied organs, except in the renal medulla. In general, the data of the renal medulla and liver had greater variation (> 25%) in all variables describing the timing (AT, TTPinj, TTPinr, Wi, and Wo), compared with the other analyzed organs.

Discussion

On the basis of results of earlier studies[17,18,30,31] with other species, typical perfusion patterns for each imaged organ were evident in the present study. The liver, which was always imaged first, had a similar pattern as seen in other species; however, TTPinj seemed to be earlier in cats, compared with dogs. The image quality was not optimal for the entire liver for 2 reasons. First, the contact between the skin of the cat and the linear probe almost always required a moderate amount of pressure, and despite the pressure, there was sometimes lack of contact in the whole field of imaging. This might cause problems in a nonanesthetized animal. Second, the probe frequency and the dosage of the contrast medium were so high that noticeable attenuation occurred in the far field (4-cm depth). Because of dual hepatic blood flow[32] and close proximity of the diaphragm, which caused more respiratory motion in the image, increased heterogeneity was visible both in the image (during the first 10 to 15 seconds) and in the time-intensity curve (during the complete 30 seconds).[31]

The renal cortex had a homogeneous, early, and intense enhancement, followed by a more gradual and heterogeneous enhancement of the medulla, which was similar to other species[4,22]; however, TTPinj seemed to be earlier in the renal cortex in cats, compared with dogs. The renal medulla seemed to have sparse enhancement, first at the periphery and then followed by gradual enhancement of the inner portions, according to the direction of blood flow.[33,34]

The pancreas, small intestine, and mesenteric lymph nodes all had an early, intense, and uniform enhancement, as could be expected in organs receiving all their blood—and therefore also microbubbles—directly from afferent arteries, which was also reported in earlier studies.[35–37] When imaging the pancreas, the scan plane and greater amount of respiratory motion resulted in more heterogeneity in the time-intensity curve.

The differences in the functional perfusion variables (Table 1) can be mostly explained by physiologic differences among the vascular structures and blood flows of the organs.[4,33,34,38,39] The impact of anesthesia on organ perfusion, however, is a confounding factor and needs to be further studied in detail. To our knowledge, the anesthetics used in combination in the present study have not been studied either separately in cats or as a combination in any species. Furthermore, vascular reactions in an organ cannot be easily estimated through cardiopulmonary and blood flow measurements alone. Brown et al[40] reported no significant changes in heart rate with long-term (6-hour) anesthesia performed with continuous infusion of guaifenesin, ketamine, and xylazine in cats. In studies[41–44] performed in other species, the cardiopulmonary and hemodynamic effects of various anesthetics have been discussed, but none of the studies have investigated the effects of the anesthetic combination used in this study. Therefore, we can only speculate what effect the anesthesia used in this study had on each organ. Despite the importance of potential anesthetic effects, however, in this study, perfusion variables were similar among the pancreas, small intestine, and mesenteric lymph nodes.

The relatively large variation in liver perfusion variables, compared with other organs, was most likely caused by small differences in regional blood flow caused by the complex vascular structure in the liver[31,39,45] and by the close proximity of the diaphragm, which caused a greater amount of motion artifact. The shape of the time-intensity curve reflects the vascular structure of a scanned organ.[31] The gentle slope of both the wash-in and wash-out phase was noticed to be typical of the liver.[17,18,45] This seemed to be attributable to the dual blood flow from the hepatic artery and portal vein.[31,32] In our study, the exact location of the ROI in the liver lobe could not be kept constant among cats. This might cause some extra variation (besides the variation caused by respiratory motion and poor image quality) in the variables because the placement of the transducer, as well as the imaged liver lobe, reportedly has an influence in the observed perfusion variables in rabbits.[31] The moderate heterogeneity observed in the perfusion pattern of the liver is, however, reportedly less than the differences between healthy liver and focal hepatic neoplastic changes observed both by qualitative and quantitative CEUS.[30,46] Therefore, it is not clinically important when comparing focal perfusional changes, but it might be confusing when detecting diffuse or milder focal changes in the liver.

The differences in perfusion variables between the renal cortex and all other organs reflect the differences in vascular structure and blood flow.[33] The renal cortex is highly vascularized with a unique, well-organized vascular structure at the level of both macro- and microcirculation.[33] The marked difference in perfusion, detected with CEUS, between the renal cortex and medulla corresponds with the physiologic features of those structures[33,34] and is in agreement with previous studies[4,20] in other species. The difference in perfusion between cortex and medulla may be overestimated, however, because the ROIs drawn in the cortex and medulla were not exactly at the same depth. This was

caused by the small size of the cranial pole of the feline kidney. The depth of the ROI has an effect on the obtained perfusion variables.[47] Also, the size of the ROIs would have been different between the cortex and medulla, if the ROI had been drawn in the cranial pole of the kidney. Both of these factors (depth and size of the ROI) can have an effect on the appearance of the time-intensity curve.[47]

The delayed onset of signal and longer time required to reach PI (gentler slope) apparent in the renal medulla, compared with the cortex, can be explained by vascular structure differences; most of the blood flow into the medulla comes through a capillary network.[33,34] The volume and velocity of the blood flow in the medulla are much less than in the cortex, and some microbubbles may have already been exposed to ultrasonography before entering the medulla.[4] The large variation detected in the perfusion variables was similar to the results of previous studies in dogs[20] and rabbits.[4] This variation can be predominantly explained by the vague and heterogeneous enhancement pattern of the medulla because of its vascular structure and differences in the regional blood flow in the outer and inner medulla.[34] The slower and lower blood flow and therefore smaller amount of circulating microbubbles cause more variation in the detected intensities in relation to time,[4] partially because of vascular heterogeneity in the medulla and partially because of a greater impact of motion artifact on the time-intensity curve. Some of this variation may, however, represent true variation among individuals. Therefore, further studies are needed to estimate its importance in clinical patients with renal disease affecting the medulla.

The subgroup of pancreas, small intestine, and mesenteric lymph nodes had similar perfusion patterns, as could have been expected because of the similarities in vascular structure among the organs (arterial afferent vessels). However, there were differences between this subgroup of organs and the liver and renal cortex in the variables describing the timing (AT, TTPinj, and TTPinr) and also in BI and PI between the liver and pancreas. The differences between the organs in the subgroup and the liver can be mostly explained by differences in the afferent vessel systems and vascular structure.[39] The differences between the organs in the subgroup and renal cortex could be explained by vascular structure and differences in blood flow.[38]

Repeatability of obtaining perfusional variables was good in both the liver and renal cortex. The difference between the 2 injections in BI in the liver data could be attributable to variation caused by respiration, the complex dual blood flow and sinusoidal blood flow,[45] differences in blood flow between separate areas of the liver,[31] or true baseline variation because of bubble uptake by the sinusoids or bubble saturation.[45] The difference observed in the BI, however, was considered clinically unimportant because it was remarkably less than the reported difference in PI between healthy and diseased liver tissue.[48]

In the renal cortex, no significant difference was found between the separate injections for any of the variables. However, the sequence of the injections was different between the liver and renal cortex because the liver was the first organ imaged (injections 1 and 2) and the cats had already had several injections before the kidney was imaged (injections 5 and 6). Therefore, a small difference in BI among cats could have been hidden by a small amount of residual microbubbles because the effect of several contrast injections on perfusion variables, and specifically BI, is not known to the best of our knowledge. Results indicated that no significant differences in the perfusion variables existed between 2 injections with the scanning intervals used in this study.

The large variation discovered in the perfusion variables of the renal medulla (AT, TTPinj, PI, TTPinr, Wi, and Wo) and the liver (AT, BI, TTPinj, TTPinr, Wi, and Wo) was probably attributable to slower, lesser, and more heterogeneous venous blood supply,[31] smaller amount of circulating microbubbles, and motion artifact, compared with other organs.[4,47] Further studies are needed to fully understand the reason and effect of this variation and to estimate its importance in clinical patients with renal medullary or diffuse liver disease.

Quantitative CEUS, however, results often in values that are not entirely comparable among studies. First, the results may vary because of the multiple factors affecting the time-intensity curve, such as technical scanning variables, contrast agent characteristics, and patient-related factors.[45,47,49,50] Second, the differences in intensity-measuring units and scales among different imaging modalities (dB vs video-intensity units) can further complicate comparisons. Furthermore, the present study was performed on anesthetized cats, and anesthesia is known to affect the perfusion of several organs. Therefore, these results must not be correlated with results in nonanesthetized patients without caution.

The present results indicate that CEUS can be used in cats to estimate organ perfusion as in other species. The obtained baseline data may serve as reference values in the future assessment of cats with kidney, liver, pancreatic, intestinal, or lymph node disease or suspected vascular compromise.

a. Acuson Sequoia 512, Siemens Medical Solutions, Mountain View, Calif.
b. CPS, Siemens Medical Solutions, Mountain View, Calif.
c. Definity, Lantheus Medical Imaging, North Billerica, Mass.
d. ACQ*syngo Auto-tracking Contrast Quantification, Acuson Sequoia C512 system, Siemens Medical Solutions, Mountain View, Calif.
e. Excel 2003, version 20.12, Microsoft Corp, Redmond, Wash.
f. Prism, version 4.01 for Windows, GraphPad Software, San Diego, Calif.
g. SPSS, version 15.0 for Windows, SPSS Inc, Chicago, Ill.
h. Statistix, version 9, Analytical Software, Tallahassee, Fla.

References

1. Nilsson A. Contrast-enhanced ultrasound of the kidneys. *Eur Radiol* 2004;14(suppl 8):P104–P109.
2. Du J, Li FH, Fang H, et al. Microvascular architecture of breast lesions: evaluation with contrast-enhanced ultrasonographic micro flow imaging. *J Ultrasound Med* 2008;27:833–842.
3. Wei K, Le E, Bin JP, et al. Quantification of renal blood flow with contrast-enhanced ultrasound. *J Am Coll Cardiol* 2001;37:1135–1140.
4. Potdevin TCU, Fowlkes JB, Moskalik AP, et al. Refill model of

rabbit kidney vasculature. *Ultrasound Med Biol* 2006;32:1331–1338.
5. Quaia E. Microbubble ultrasound contrast agents: an update. *Eur Radiol* 2007;17:1995–2008.
6. Claudon M, Cosgrove D, Albrecht T, et al. Guidelines and good clinical practice recommendations for contrast enhanced ultrasound (CEUS)—update 2008. *Ultraschall Med* 2008;29:28–44.
7. Martegani A, Aiani L, Borghi C. The use of contrast-enhanced ultrasound in large vessels. *Eur Radiol* 2004;14(suppl 8):P73–P86.
8. Thorelius L. Contrast-enhanced ultrasound in trauma. *Eur Radiol* 2004;14(suppl 8):P43–P52.
9. Solbiati L, Ierace T, Tonolini M, et al. Guidance and monitoring of radiofrequency liver tumor ablation with contrast-enhanced ultrasound. *Eur J Radiol* 2004;51(suppl):S19–S23.
10. Nicolau C, Catala V, Vilana R, et al. Evaluation of hepatocellular carcinoma using SonoVue, a second generation ultrasound contrast agent: correlation with cellular differentiation. *Eur Radiol* 2004;14:1092–1099.
11. Burns PN, Wilson SR. Focal liver masses: enhancement patterns on contrast-enhanced images—concordance of US scans with CT scans and MR images. *Radiology* 2007;242:162–174.
12. Dietrich CF, Kratzer W, Strobe D, et al. Assessment of metastatic liver disease in patients with primary extrahepatic tumors by contrast-enhanced sonography versus CT and MRI. *World J Gastroenterol* 2006;12:1699–1705.
13. Mehran R, Nikolsky E. Contrast-induced nephropathy: definition, epidemiology, and patients at risk. *Kidney Int Suppl* 2006;(100):S11–S15.
14. Perazella MA. Gadolinium-contrast toxicity in patients with kidney disease: nephrotoxicity and nephrogenic systemic fibrosis. *Curr Drug Saf* 2008;3:67–75.
15. Ohlerth S, Scharf G. Computed tomography in small animals—basic principles and state of the art applications. *Vet J* 2007;173:254–271.
16. LeBlanc AK, Daniel GB. Advanced imaging for veterinary cancer patients. *Vet Clin North Am Small Anim Pract* 2007;37:1059–1077.
17. Ziegler LE, O'Brien RT, Waller KR, et al. Quantitative contrast harmonic ultrasound imaging of normal canine liver. *Vet Radiol Ultrasound* 2003;44:451–454.
18. Nyman HT, Kristensen AT, Kjelgaard-Hansen M, et al. Contrast-enhanced ultrasonography in normal canine liver. Evaluation of imaging and safety parameters. *Vet Radiol Ultrasound* 2005;46:243–250.
19. Ohlerth S, Ruefli E, Poirier V, et al. Contrast harmonic imaging of the normal canine spleen. *Vet Radiol Ultrasound* 2007;48:451–456.
20. Waller KR, O'Brien RT, Zagzebski JA. Quantitative contrast ultrasound analysis of renal perfusion in normal dogs. *Vet Radiol Ultrasound* 2007;48:373–377.
21. Nakamura K, Sasaki N, Yoshikawa M, et al. Quantitative contrast-enhanced ultrasonography of canine spleen. *Vet Radiol Ultrasound* 2009;50:104–108.
22. Rademacher N, Ohlerth S, Scharf G, et al. Contrast-enhanced power and color Doppler ultrasonography of the pancreas in healthy and diseased cats. *J Vet Intern Med* 2008;22:1310–1316.
23. Blomley M, Claudon M, Cosgrove D. WFUMB safety symposium on ultrasound contrast agents: clinical applications and safety concerns. *Ultrasound Med Biol* 2007;33:180–186.
24. Piscaglia F, Bolondi L. Italian Society for Ultrasound in Medicine and Biology (SIUMB) Study Group on Ultrasound Contrast Agents. The safety of Sonovue in abdominal applications: retrospective analysis of 23188 investigations. *Ultrasound Med Biol* 2006;32:1369–1375.
25. O'Brien RT, Iani M, Matheson J, et al. Contrast harmonic ultrasound of spontaneous liver nodules in 32 dogs. *Vet Radiol Ultrasound* 2004;45:547–553.
26. Kutara K, Asano K, Kito A, et al. Contrast harmonic imaging of canine hepatic tumors. *J Vet Med Sci* 2006;68:433–438.
27. Rossi F, Leone VF, Vignoli M, et al. Use of contrast-enhanced ultrasound for characterization of focal splenic lesions. *Vet Radiol Ultrasound* 2008;49:154–164.
28. Ohlerth S, Dennler M, Ruefli E, et al. Contrast harmonic imaging characterization of canine splenic lesions. *J Vet Intern Med* 2008;22:1095–1102.
29. Ivancic M, Long F, Seiler GS. Contrast harmonic ultrasonography of splenic masses and associated liver nodules in dogs. *J Am Vet Med Assoc* 2009;234:88–94.
30. Quaia E, Palumbo A, Rossi S, et al. Comparison of visual and quantitative analysis for characterization of insonated liver tumors after microbubble contrast injection. *AJR Am J Roentgenol* 2006;186:1560–1570.
31. Li J, Dong BW, Yu XL, et al. Gray scale contrast enhancement and quantification in different positions of rabbit liver. *J Ultrasound Med* 2006;25:7–14.
32. Lueck GJ, Kim TK, Burns PN, et al. Hepatic perfusion imaging using factor analysis of contrast enhanced ultrasound. *IEEE Trans Med Imaging* 2008;27:1449–1457.
33. Hollenberg N. The physiology of the renal circulation. In: Black D, Jones N, eds. *Renal disease*. 4th ed. Oxford, England: Blackwell Mosby Book Distributions, 1979;30–63.
34. Pallone TL, Zhang Z, Rhinehart K. Physiology of the renal medullary microcirculation. *Am J Physiol Renal Physiol* 2003;284:F253–F266.
35. D'Onofrio M, Zamboni G, Faccioli N, et al. Ultrasonography of the pancreas. 4. Contrast-enhanced imaging. *Abdom Imaging* 2007;32:171–181.
36. Mitsuoka Y, Hata J, Haruma K, et al. New method of evaluating gastric mucosal blood flow by ultrasound. *Scand J Gastroenterol* 2007;42:513–518.
37. Rubaltelli L, Khadivi Y, Tregnaghi A, et al. Evaluation of lymph node perfusion using continuous mode harmonic ultrasonography with a second-generation contrast agent. *J Ultrasound Med* 2004;23:829–836.
38. Geboes K, Geboes KP, Maleux G. Vascular anatomy of the gastrointestinal tract. *Best Pract Res Clin Gastroenterol* 2001;15:1–14.
39. McCuskey RS. The hepatic microvascular system in health and its response to toxicants. *Anat Rec (Hoboken)* 2008;291:661–671.
40. Brown MJ, McCarthy TJ, Bennett BT. Long term anesthesia using a continuous infusion of guaifenesin, ketamine and xylazine in cats. *Lab Anim Sci* 1991;41:46–50.
41. Hobbs BA, Rolhall TG, Sprenkel TL, et al. Comparison of several combinations for anesthesia in rabbits. *Am J Vet Res* 1991;52:669–674.
42. Magoon KE, Hsu WH, Hembrough FB. The influence of atropine on the cardiopulmonary effects of a xylazine-ketamine combination in dogs. *Arch Int Pharmacodyn Ther* 1988;293:143–153.
43. Kolata RJ, Rawlings CA. Cardiopulmonary effects of intravenous xylazine, ketamine, and atropine in the dog. *Am J Vet Res* 1982;43:2196–2198.
44. Wright M. Pharmacologic effects of ketamine and its use in veterinary medicine. *J Am Vet Med Assoc* 1982;180:1462–1471.
45. Li J, Dong B, Yu X, et al. Grey-scale contrast enhancement in rabbit liver with SonoVue at different doses. *Ultrasound Med Biol* 2005;31:185–190.
46. Wang Z, Tang J, An L, et al. Contrast-enhanced ultrasonography for assessment of tumor vascularity in hepatocellular carcinoma. *J Ultrasound Med* 2007;26:757–762.
47. Mule S, De Cesare A, Lucidarme O, et al. Regularized estimation of contrast agent attenuation to improve the imaging of microbubbles in small animal studies. *Ultrasound Med Biol* 2008;34:938–948.
48. Bartolotta TV, Midiri M, Scialpi M, et al. Focal nodular hyperplasia in normal and fatty liver: a qualitative and quantitative evaluation with contrast-enhanced ultrasound. *Eur Radiol* 2004;14:583–591.
49. Sonne C, Xie F, Lof J, et al. Differences in definity and optison microbubble destruction rates at a similar mechanical index with different real-time perfusion systems. *J Am Soc Echocardiogr* 2003;16:1178–1185.
50. Porter TR, Kricsfeld D, Cheatham S, et al. The effect of ultrasound frame rate on perfluorocarbon-exposed sonicated dextrose albumin microbubble size and concentration when insonifying at different flow rates, transducer frequencies, and acoustic outputs. *J Am Soc Echocardiogr* 1997;10:593–601.